communications biology

Article

https://doi.org/10.1038/s42003-024-07310-2

Two outbreak cases involving ST65-KL2 and ST11-KL64 hypervirulent carbapenem-resistant *Klebsiella pneumoniae*: similarity and diversity analysis

Feilong Zhang[1,2], Zhihua Li[2,3], Ziyao Li[1,2], Xinmeng Liu[2], Zichen Lei[2,4], Xianxia Zhuo[2,5], Xinrui Yang[1,2], Jiankang Zhao[2], Yulin Zhang[2] & Binghuai Lu[1,2,3,4] ✉

The rise of the convergence of hypervirulence and carbapenem resistance in *Klebsiella pneumoniae* has been increasingly reported in recent years, however, there are few outbreak cases for these producing NDM carbapenemase. In this study, ST65-KL2 and ST11-KL64 hypervirulent and carbapenem-resistant *K. pneumoniae* (hvCRKP) were identified from two different outbreak cases: (1) clonal spreading of ST65-KL2 in five patients within transplantation wards spanning three months; and (2) clonal transmission of ST11-KL64 in ten patients across 10 months. The representative strains of ST65-KL2 and ST11-KL64 hvCRKP, K22877 and K56649, produced carbapenemase NDM-5 and dual carbapenemases KPC-2 and NDM-13, respectively, and both exhibited high-level carbapenem resistance. Moreover, virulent analysis showed that K22877 and K56649 were hypervirulent and the former possessed stronger virulence. Evolutionary pathways suggested ST65-KL2 and ST11-KL64 hvCRKP could be classified as CR-hvKP (hvKP acquiring carbapenem resistance) and hv-CRKP (CRKP acquiring hypervirulence), respectively. Unexpectedly, ST65-KL2 CR-hvKP showed resistance to ciprofloxacin mediated by plasmid acquisition as its spread, and ST11-KL64 hv-CRKP developed into enhanced virulence and macrophage resistance. Furthermore, compared to the ST65-KL2 CR-hvKP, the ST11-KL64 hv-CRKP tends to cause occult and persistent infection. Global genome analysis revealed ST11-KL64 hv-CRKP and ST65-KL2 CR-hvKP mainly carried bla_{KPC-2} and had significant differences in Ompk35/36, *ybt*, resistance and virulence. Effective surveillance should be implemented and novel therapeutic strategies are urgently needed to deal with refractory infections.

Klebsiella pneumoniae is a notorious opportunistic pathogen causing approximately a third of all Gram-negative bacterial infections, including bloodstream infection, pneumonia and urinary tract infection, with high morbidity and mortality[1–3]. Conventionally, it was divided into two groups: hypervirulent *K. pneumoniae* (hvKP) possessing high pathogenicity and capable of causing community-acquired infections, mainly in immunocompetent individuals, and classical *K. pneumoniae* (cKP) easily obtaining multi-drug resistance (MDR) and

[1]Peking Union Medical College, Chinese Academy of Medical Sciences, China-Japan Friendship Hospital, Beijing, China. [2]National Center for Respiratory Medicine, State Key Laboratory of Respiratory Health and Multimorbidity, National Clinical Research Center for Respiratory Diseases, Institute of Respiratory Medicine, Chinese Academy of Medical Sciences, Laboratory of Clinical Microbiology and Infectious Diseases, Department of Pulmonary and Critical Care Medicine, Center of Respiratory Medicine, China-Japan Friendship Hospital, Beijing, China. [3]Peking University China-Japan Friendship School of Clinical Medicine, Beijing, China. [4]China-Japan Friendship Institute of Clinical Medical Sciences, Beijing, China. [5]Department of Pulmonary and Critical Care Medicine, Capital Medical University, Beijing, China. ✉e-mail: zs25041@126.com

mainly resulting in nosocomial infections in immunocompromised patients[4].

Compared to cKP, hvKP exhibits some hypervirulent features, such as capsule loci types (KL1 and KL2) and virulence plasmids (pLVPK and pK2044), usually shows hypermucoviscosity by string test and sensitivity to most antibiotics, and produces more capsular polysaccharides (CPS) and siderophore[4]. Furthermore, virulence plasmids usually harbor mucoid regulator genes (*rmpADC* or *rmpA2*), aerobactin genes (*iutAiucABCD*) and salmochelin genes (*iroBCDN*)[5]. However, the definition of hvKP remains ambiguous, as likely to cause excessive reporting in hvKP[6]. cKP will be easier to acquire resistance phenotypes than hvKP, owing to its lack of thick CPS, which contributes to the rise of carbapenem- and polymyxin-resistant cKP, individually or simultaneously. They commonly belong to sequence type (ST) 258, ST11, ST512, ST307 and ST15[7,8].

Furthermore, the increase of carbapenem-resistant *K. pneumoniae* (CRKP), largely due to carbapenemase production, become a global and serious threat to public health[9]. KPC, NDM and OXA-48 are the most popular carbapenemases for CRKP globally, and outbreak cases of CRKP harbored those carbapenemases have been documented in Europe, Asia, America, causing trouble with prevention and control[10–12].

What is noteworthy is that the convergence of hypervirulent and carbapenem-resistant *K. pneumoniae* (hvCRKP) has occurred and showed great potential to cause difficult-to-treat infections[13]. Those strains might be generated in the following three pathways: CRKP acquiring hypervirulence (hv-CRKP), hvKP acquiring carbapenem resistance (CR-hvKP) and cKP acquiring both hypervirulence and carbapenem resistance (hvCR-KP). hv-CRKP, CR-hvKP and hvCR-KP isolated from patients have been sporadically reported within the last five years, such as ST11-KL64/KL47 hv-CRKP, ST23-KL1/ ST86-KL2 CR-hvKP and ST11-KL64 hvCR-KP[14,15]. The bla_{KPC}-containing hvCRKP has been reported; however, there is limited data on bla_{NDM}-harboring hvCRKP and its outbreaks[16].

In the present study, to the best of our knowledge, we first reported two different types of fatal outbreaks, caused by ST11-KL64 hv-CRKP co-carrying bla_{KPC-2} and bla_{NDM-13} and ST65-KL2 CR-hvKP carrying bla_{NDM-5} in intensive care units (ICUs) and transplantation wards of a tertiary hospital from March 2023 to December 2023 and May 2019 to August 2019, respectively, in China. Whole-genome sequencing (WGS) and a series of phenotypic experiments were performed for the in-depth understanding of the above two clonal outbreaks. Dynamic evolutions of resistance and virulence were also identified in the process of dissemination. Furthermore, a thorough comparison of the genomic and clinical characteristics of the above two types of hvCRKP was also carried out.

Results

Two outbreaks of hvCRKP spreading rapidly but latently

The emergence and spread of carbapenemase-producing hvCRKP were identified by antibiotic sensitivity testing (AST), APB (3-aminophenylboronic acid) and EDTA enhancement method (APB/EDTA method), polymerase chain reaction (PCR) and WGS. In the present study, since June 2019, 15 hvCRKP strains were collected from five patients, including three kidney transplant recipients and two lung recipients, within three months (Fig. 1 and Table 1), and these belonged to the same cluster confirmed by Xbal-PFGE, cgMLST and phylogenetics (Figs. 2A, S1 and S5), revealing the outbreak of hvCRKP occurred during transplantation and hospitalization due to the monophyletic spread. Moreover, the isolation and hospitalization timelines for those hvCRKP strains revealed they derived from the two lungs and kidneys of the same donor, respectively, and then disseminated in the same ward due to close contact (Figs. 1 and 2B). Fortunately, aztreonam was an effective remedy for combating the hvCRKP and shortening the course of the disease. However, the severe complications after lung transplantation in Patients 1-1 and 1-2 brought them into critical condition, and they died in two weeks.

Another outbreak case was caused by ST11-KL64 hvCRKP, the most prominent ST-KL in China, which was first discovered in the blood and bronchoalveolar lavage fluid (BALF) of a patient suffering from acute exacerbation of chronic obstructive pulmonary disease and resulted in septic shock and death. The hvCRKP, co-carrying bla_{KPC-2} and bla_{NDM-13}, attracted our great attention owing to its hypervirulence and MDR. Over the following ten months, the hvCRKP was sequentially isolated from nine patients with kidney transplantation, tumor, cholangitis and intracerebral hemorrhage (Table 1). All 21 ST11-KL64 hvCRKP, five chains of clonal transmission, were categorized into a single cluster by the same methods as the ST65-KL2 hvCRKP (Fig. 2A). Treatment effectiveness against the ST11-KL64 hvCRKP was limited, which caused recurrent infections and death, although the strains showed sensitivity to the combination of aztreonam and ceftazidime-avibactam (ATM-CZA). Patients 2-2, 2-3, 2-4, 2-6, 2-8, and 2-10 suffering chronic renal failure have undergone kidney transplantation in the same ward, and had close contact in time and space within seven months, implying nosocomial spread (Figs. 1 and 2B). Of note, occult infections due to the retention of hvCRKP in Patients 2-2 and 2-6 have existed during the initial hospitalization and both appeared clinical infective symptoms in post-discharge. Interestingly, after admission, hvCRKP was immediately isolated from four patients, Patients 2-1, 2-5, 2-7 and 2-9, hinting that hvCRKP have disseminated regionally.

Resistance phenotype and molecular characterization of hvCRKP

ST11-KL64 hvCRKP strain K56649 and ST65-KL2 hvCRKP strain K22877 were taken as the representative strains for further multidrug resistance research.

AST showed ST11-KL64 K56649 expressed resistance to most beta-lactam antibiotics, including carbapenems, aztreonam and CZA, aminoglycosides, fluoroquinolones and sulfamethoxazole and trimethoprim (SXT), but was sensitive to colistin and tigecycline (Table 2). A series of resistance genes were detected in K56649 by WGS and were consistent with resistance phenotypes to beta-lactams (bla_{KPC-2}, bla_{NDM-13}, $bla_{CTX-M-65}$, bla_{TEM-1B} and bla_{LAP-2}), aminoglycosides (*rmtB*), fluoroquinolones (*qnrS1*) and SXT (*dfrA14*, *sul1* and *sul2*). Nanopore sequencing and S1-PFGE revealed K56649 harbored one chromosome and five plasmids, designated as pK56649-1, pK56649-2-KPC, pK56649-3-VIR, pK56649-4-NDM and pK56649-5 (Table S1). Replicons of those plasmids were ColRNAI, IncFII(pHN7A8)/IncR, IncHI1B/IncFIB(K), IncI1 and undetected replicon, respectively. pK56649-2-KPC harbored bla_{KPC-2} and its replicon was popular in bla_{KPC-2}-carrying plasmids. The surrounding environment of bla_{KPC-2}, located on an IncFII(pHN7A8)/IncR plasmid pK56649-2-KPC, was IS*26*-*hp*-*hp*-*klcA*-*korC*-ΔIS*Kpn6*-bla_{KPC-2}-IS*Kpn27*-Tn*3*$_{tnpR}$-IS*26*, which shared the core structure with two of the most popular bla_{KPC-2}-harboring genetic environments in China, United States and Europe, Tn*1721*-based structure and Tn*4401* (Fig. 3A). As previously reported, the bla_{KPC-2}-harboring environment has a potential spread to other plasmids in the same strains by two sides of IS*26* *via* transposable recombination, although transposable elements released inside the cytoplasm were not found[17]. Another carbapenemase gene bla_{NDM-13} was carried by IncI1 plasmid pK56649-4-NDM and first reported in plasmid pIOMTU558-NDM of *Escherichia coli*. To the best of our knowledge, bla_{NDM-13} harbored by *K. pneumoniae*, was first found in this study. Importantly, plasmid pNDM13-SR33 of *Salmonella enterica* SR33 was identical to pK56649-4-NDM (Fig. 3B), which suggested pK56649-4-NDM might be transferred to *K. pneumoniae* from *S. enterica*. Compared to NDM-1, NDM-13 with two substitutions (D95N and M154L, Fig. S2) displayed significant hydrolytic activity against cefotaxime and no changes for carbapenems. Genetic environment of bla_{NDM-13} was IS*1294*-ΔIS*Aba125*-bla_{NDM-13}-Δble_{MBL}-*trpF*. Two specific opposite sequences (CTTG) flanking IS*1294* revealed IS*1294* inserted IS*Aba125* by rolling-circle transposition. Moreover, the downstream sequence of bla_{NDM-13} also existed many characteristic target sites (GTTC), probably indicating bla_{NDM-13} was mobilized by IS*1294*, as previously reported[18]. Furthermore, conjugative prediction and conjugation experiments showed bla_{NDM-13}-harboring pK56649-4-NDM have complete conjugative regions and capability of spread to *K. pneumoniae* KP54 and *E. coli* J53 (Fig. S3). However, bla_{KPC-2} only could be transferred to *K. pneumoniae* KP54 with the help of pK56649-

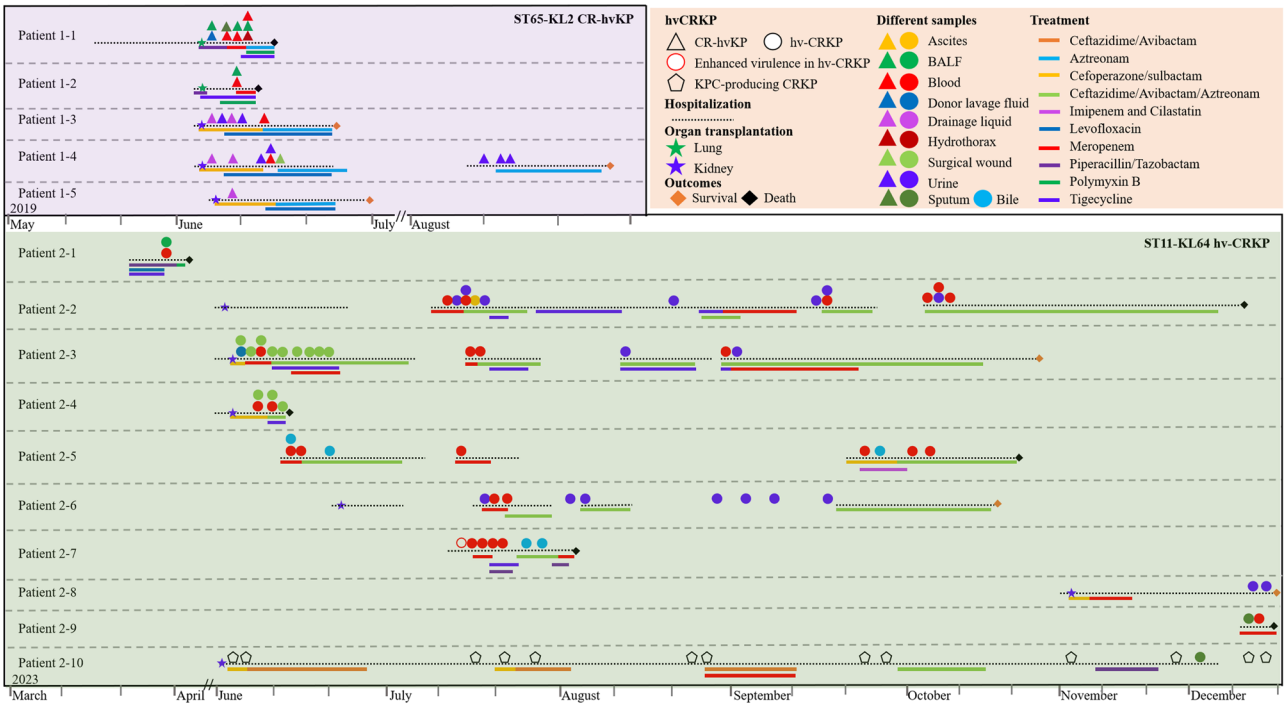

Fig. 1 | Hospitalization, isolation of hvCRKP, antibiotic treatment and clinical outcomes of fifteen patients.

Table 1 | Clinic characteristics of patients infected by hvCRKP

Strains	Patients	Age (Y)	Gender	Diseases	Ward	Invasive procedures	Province	Clinical outcomes	Isolation strains
ST65-KL2 CR-hvKP	Patient 1-1	68	Male	ILD	Lung transplant	Lung transplant	Beijing	Death	K22877, K22937, K23005, K22866, K23025
	Patient 1-2	63	Male	ILD	ICU	Lung transplant	Beijing	Death	K22972, K22974
	Patient 1-3	30	Male	CRF	Urology	Kidney transplant	Zhejiang	Recovered	K22869, K22915, K23036
	Patient 1-4	58	Male	CRF	Urology	Kidney transplant	Zhejiang	Recovered	K22900, K23016, K23033, K23102
	Patient 1-5	62	Male	CRF	Urology	Kidney transplant	Beijing	Recovered	K22994
ST11-KL64 hv-CRKP	Patient 2-1	50	Male	COPD	ICU	–	Heilongjiang	Death	K56765, K56649
	Patient 2-2	41	Male	CRF	Urology	Kidney transplant	Beijing	Death	K60217, K60216, K60395
	Patient 2-3	56	Male	CRF	Urology	Kidney transplant	Shandong	Recovered	K59116, K59005, K59194, K59052
	Patient 2-4	48	Male	CRF	Urology	Kidney transplant	Beijing	Death	K59107, K59051
	Patient 2-5	75	Male	Malignant tumor	Digestive department	ERCP	Beijing	Death	K59198, K59199
	Patient 2-6	59	Male	CRF	Urology	Kidney transplant	Beijing	Recovered	K60488, K60490
	Patient 2-7	83	Male	AOSC	ICU	PTCD	Beijing	Death	K60365, K60406
	Patient 2-8	60	Female	CRF	Urology	Kidney transplant	Hebei	Recovered	K67189
	Patient 2-9	56	Male	ICH and HAP	ICU	–	Beijing	Death	K66462, K66381
	Patient 2-10	58	Male	CRF	Urology	Kidney transplant	Beijing	Recovered	K65921

hvCRKP hypervirulent and carbapenem-resistant *K. pneumoniae*, *ILD* interstitial pulmonary disease, *CRF* chronic renal failure, *COPD* chronic obstructive pulmonary disease, *AOSC* acute obstructive suppurative cholangitis, *ICH* intracerebral hemorrhage, *HAP* hospital acquired pneumonia, *ERCP* endoscopic retrograde cholangio-pancreatography, *PTCD* percutaneous transhepatic cholangial drainage.

4-NDM by plasmid transfer since pK56649-2-KPC lacked the genes encoding relaxase and type IV coupling protein (T4CP).

Compared to ST11-KL64 hvCRKP strain K56649, ST65-KL2 strain K22877 remained susceptible to aztreonam, aminoglycosides and quinolones, which offered more choices to combat infections. bla_{NDM-5} was the only β-lactamase resistance gene identified in K22877 using WGS (Table 2), as might explain why it was sensitive to aztreonam. Moreover, genome analysis revealed that K22877 carried one chromosome and two plasmids, named pK22877-1-VIR and pK22877-2-NDM, belonging to IncFIB(K)/IncHI1B and IncX3, respectively. pK22877-2-NDM harbored bla_{NDM-5} and

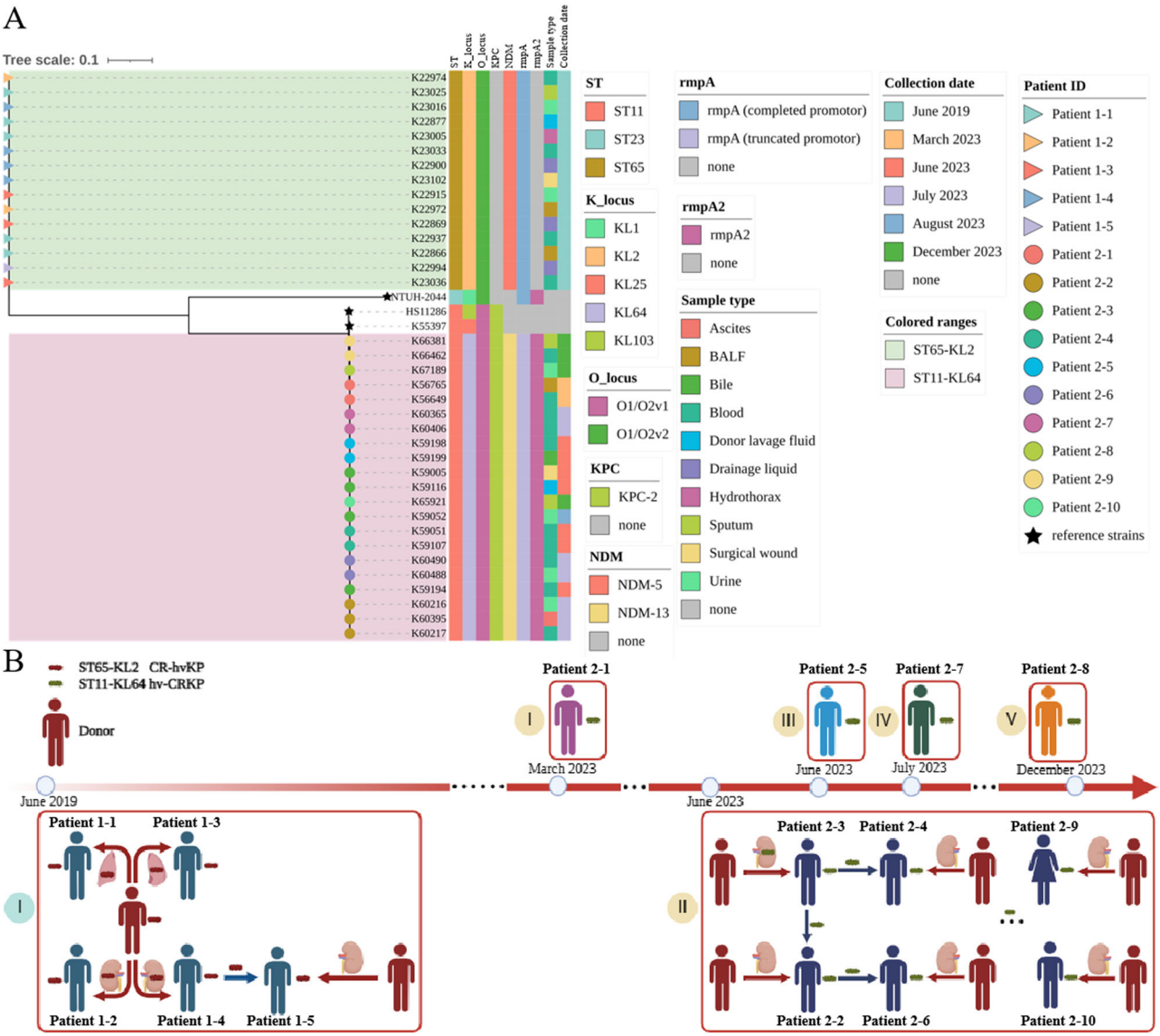

Fig. 2 | Clustering and dissemination of hvCRKP. A Phylogenetic relatedness of the hv-CRKP ($n = 21$), CR-hvKP ($n = 15$) and reference strains (hvKP NTUH-2044 and two CRKP, HS11286 and K55397) was illustrated. Patient ID, clustering, ST, K_locus, O_locus, KPC, NDM, *rmpA*, *rmpA2*, sample type and collection date were annotated in the outbreak clone. ST sequence type, KPC *K. pneumoniae* carbapenemases, NDM New Delhi metallo-β-lactamases. **B** Timeline of outbreaks of two different hvCRKP. The left showed one chain of clonal spreading of ST65-KL2 CR-hvKP and the right showed five chains of clonal dissemination of ST11-KL64 hv-CRKP. Different chains of clonal transmission were identified by collection date of strains, initial inpatient department, bed location and transplantation surgery. The Fig. 2B was created with BioRender.com by us, and its icons derived from BioRender.

its replicon was a common replicon of bla_{NDM}-harboring plasmid in *Enterobacteriales*. Moreover, the genetic environment of bla_{NDM-5} was ΔIS*3000*-IS*5*-ΔIS*Aba125*-bla_{NDM-5}-ble_{MBL}-*trpF*-*dsbD*-Δ*cutA*-IS*26*-IS*Kox3*. Conjugation assays indicated pK22877-2-NDM carrying bla_{NDM-5} could be transferred to *E. coli* J53 and *K. pneumoniae* KP54, identified by PCR, to cause the spread of carbapenem resistance (Fig. S3).

Molecular and phenotypic characterizations of hypervirulence in ST11-KL64 and ST65-KL2 hvCRKP

Genomic analysis indicated all ST11-KL64 ($n = 21$) and ST65-KL2 ($n = 15$) hvCRKP harbored hypervirulent-like plasmid, pK56649-3-VIR and pK22877-1-VIR, respectively. The two hypervirulent-like plasmids have >90% coverage and >99% identity with the typical hypervirulent plasmid pLVPK and pK2044 (Fig. 3C). Replicons of the four plasmids were identical and belonged to IncHI1B/IncFIB. pK22877-1-VIR carried a series of hypervirulent markers, including *rmpA*, *iutA*i*ucABCD* and *iroBCDN*, the same as pLVPK and pK2044 (Table S1).

Compared to pK22877-1-VIR, pK56649-3-VIR did carry *rmpA*, *rmpA2* and *iutA*i*ucABCD*, but did not carry *iroBCDN*. Interestingly, the promotor of *rmpA* in plasmid pK56649-3-VIR, was truncated by IS*Kpn26* in the position -6 region of *rmpA*, causing the block of transcription (Fig. S4).

Likely, the same truncations in ST11-KL64 strains of spread chains I, II and V were found. Of note is that the promotor of *rmpA* in ST11-KL64 strains of spread chain III and IV was cut off by IS*Kpn74* in –2 region of *rmpA* except for K60365 of chain IV. The promotor of *rmpA* of K60365 showed deletion of 2802 bp in –2 region of *rmpA*. However, the *rmpA2* and its promoter in the ST11-KL64 hvCRKP were intact, compared to the incomplete promotor of *rmpA*. The *rmpA2* was identical to that of pK2044, a hypervirulent plasmid of KL1 hvKP, which significantly enhanced hypervirulence in *K. pneumoniae*. Opposite to pK56649-3-VIR, pK22877-1-VIR harbored a complete and wild promotor P_{11T} of *rmpA*, and did not contain *rmpA2*. Additionally, K22877 and K56649 contained other virulence factors located in chromosome, including *mrkABCDFHIJ*,

Table 2 | Resistance phenotypes and genotypes and virulence genes of *Klebsiella pneumoniae* and its transconjugants

Strains[a]	Species	Carbapenemase genes	Virulence genes	Minimal inhibitory concentration[b] (MIC, mg/L)							
				IPM	MEM	ATM	AMK	CZA	ATM/A	TGC	CST	CIP
K22877	*K. pneumoniae*	bla_{NDM-5}	*rmpA*, *rmpA2*, *iutAiucABCD* and *iroBCDN*	**≥16**	**≥16**	≤1	≤2	**≥256**	0.5	≤0.5	≤0.5	≤0.25
K23016	*K. pneumoniae*	bla_{NDM-5}	*rmpA*, *rmpA2*, *iutAiucABCD* and *iroBCDN*	**≥16**	**≥16**	≤1	≤2	**≥256**	0.5	≤0.5	≤0.5	**≥4**
J53	*E. coli*	–	–	≤0.25	≤0.25	≤1	≤2	≤0.125	≤0.125	≤0.5	≤0.5	–
J53-K22877-T	*E. coli*	bla_{NDM-5}	–	**≥16**	**≥16**	≤1	≤2	**≥256**	0.5	≤0.5	≤0.5	–
KP54	*K. pneumoniae*	–	–	≤0.25	≤0.25	**≥64**	**≥64**	≤0.125	≤0.125	2	≤0.5	–
KP54-K22877-T	*K. pneumoniae*	bla_{NDM-5}		**≥16**	**≥16**	**≥64**	**≥64**	**≥256**	≤0.125	2	≤0.5	–
K56649	*K. pneumoniae*	bla_{KPC-2}, bla_{NDM-13}	*rmpA*(promotor truncated), *rmpA2* and *iutAiucABCD*	**≥16**	**≥16**	**≥64**	**≥64**	**≥256**	0.5	≤0.5	≤0.5	**≥4**
K60365	*K. pneumoniae*	bla_{KPC-2}, bla_{NDM-13}	*rmpA*(promotor truncated), *rmpA2* and *iutAiucABCD*	**≥16**	**≥16**	**≥64**	**≥64**	**≥256**	0.5	≤0.5	≤0.5	**≥4**
KP54- K56649-T1	*K. pneumoniae*	bla_{NDM-13}	–	**≥16**	**≥16**	**≥64**	**≥64**	**≥256**	0.25	2	≤0.5	–
KP54- K56649-T2	*K. pneumoniae*	bla_{KPC-2}, bla_{NDM-13}	–	**≥16**	**≥16**	**≥64**	**≥64**	**≥256**	0.5	2	≤0.5	–
J53- K56649-T	*E. coli*	bla_{NDM-13}	–	**≥16**	**≥16**	**≥64**	**≥64**	**≥256**	0.25	2	≤0.5	–

[a] *K. pneumoniae* K22877 and K23016 belonged to ST65-KL2 CR-hvKP, and K56649 and K60365 belonged to ST11-KL64 hv-CRKP. J53 and KP54 were the recipients for conjugation. J53-K22877-T, KP54- K56649-T1, KP54- K56649-T2 and J53- K56649-T3 belonged to hvCRKP[+] transconjugants.

[b] IMP, imipenem; MEM, meropenem; ATM, aztreonam; AMK, amikacin, CZA, ceftazidime/avibactam; ATM/A, aztreonam/avibactam; TGC, tigecycline; CST, colistin; CIP, ciprofloxacin. The bold values indicate the MICs mean resistance.

fimABCDEFGHIK, complete iron uptake system (*entABCDEFS*, *fepABCDG*) and a series of T6SS genes.

To verify the hypervirulence of two hvCRKP, a battery of phenotype experiments was carried out. K22877 was found to be hypermucoviscous by string test in a blood plate medium, whereas K56649 was not. *G. mellonella* infection model and murine model were performed to identify the virulence of K56649 and K22877(Fig. 4A–C). Analysis suggested mortality of the larvae (injection with 1×10^5 CFU) and the mice (injection with 2×10^7 CFU) infected with K56649 and K22877, respectively, was significantly higher compared to hypovirulent strain ATCC 700603 ($P < 0.01$), and comparable to hypervirulent strain NTUH-K2044 ($P > 0.05$), using Kaplan–Meier survival curve, which implied K56649 and K22877 were hypervirulent CRKP.

Evolutionary pathways of ST11-KL64 and ST65-KL2 hypervirulent CRKP

The KPC-2- and NDM-13-producing hvCRKP belonged to ST11-KL64, a classical ST-KL of cKP, and kept a closer phylogenetic distance with cKP but not hvKP (Fig. 2A). Therefore, the ST11-KL64 hvCRKP might have originated from cKP, not hvKP. Moreover, homological plasmids with pK56649-2-KPC hinted almost of all plasmids, dating back to 2010, were carried by *K. pneumoniae*, and most of them carried bla_{KPC-2} and were isolated from China (Fig. 3D). On the contrary, the homology plasmids of pK56649-4-NDM were carried by other Gram-negative bacteria, mainly including *E. coli*, *S. enterica*, but not *K. pneumoniae*, and from Europe, America, Asia, and Africa, tracing back to 1976 (Fig. 3E). Two of those homology plasmids also harbored bla_{NDM-13}, including an identical plasmid pNDM13-SR33 (CP092912.1) in *S. enterica* with pK56649-4-NDM. In addition, conjugation experiments verified pK56649-4-NDM was a self-conjugative plasmid, and pK56649-2-KPC, a non-self-conjugative plasmid, could be mobilized with the help of pK56649-4-NDM. Therefore, we inferred pK56649-4-NDM probably originated from *S. enterica*, and pK56649-2-KPC was acquired earlier than pK56649-4-NDM for the hvCRKP co-carrying bla_{KPC-2} and bla_{NDM-13}. Owing to the considerable existence of ST11-KL64 bla_{KPC-2}-carrying hv-CRKP, hypervirulent plasmid pK56649-3-VIR was obtained after acquiring pK56649-2-KPC or pK56649-4-NDM. Moreover, strain 16ZR-60 (GCF_016750625.1), isolated from pus in Hong Kong, carried bla_{KPC-2} and the same virulent genes with K56649, and is the closest relative to K56649, only 317 SNPs difference (Fig. S6). In summary, the above analysis showed ST11-KL64 hvCRKP belonged to hv-CRKP and pK56649-2-KPC was obtained prior to pK56649-4-NDM (Fig. S3).

Compared to hv-CRKP, the ST65-KL2 hvCRKP carrying pLVPK-like plasmid, belonged to mainstream ST of hvKP and was classified as hvKP by clustering with representative hvKP, which indicated pK22877-2-NDM was obtained by the hvKP and the hvCRKP was CR-hvKP. More than five hundred homology plasmids of the pK22877-2-NDM were identified on NCBI and mainly harbored in *E. coli* (46.0%) and *K. pneumoniae* (21.0%). Of note, the IncX3 bla_{NDM-5}-carrying plasmid pK22877-2-NDM showed no difference in size and structure with seven plasmids in *Klebsiella spp.*, *E. coli*, *E. hormaechei* and *Raoultella ornithinolytica* from human and poultry in different countries, including America, Australia, China and Denmark, which showed that bla_{NDM-5}-harboring IncX3 plasmid could transfer between different species and have spread worldwide.

Therefore, ST11-KL64 hvCRKP and ST65-KL2 hvCRKP belonged to hv-CRKP and CR-hvKP, respectively, from the opposite evolutionary pathways (Fig. S3).

Virulence evolution of ST11-KL64 hv-CRKP and resistance evolution of ST65-KL2 CR-hvKP

Interestingly, K60365, another ST11-KL64 hv-CRKP, was isolated from the blood of the patient 2-7, and showed a positive string test in China blue agar, compared with K56649 (Fig. S7). Mucoviscosity, relative thickness of bacterial capsular and uronic acids also revealed that K60365 possessed more CPS than K56649 ($P < 0.0001$, $P < 0.01$, and $P < 0.001$, respectively, Fig. 4D–F). Moreover, K60365 exhibited stronger resistance to macrophage

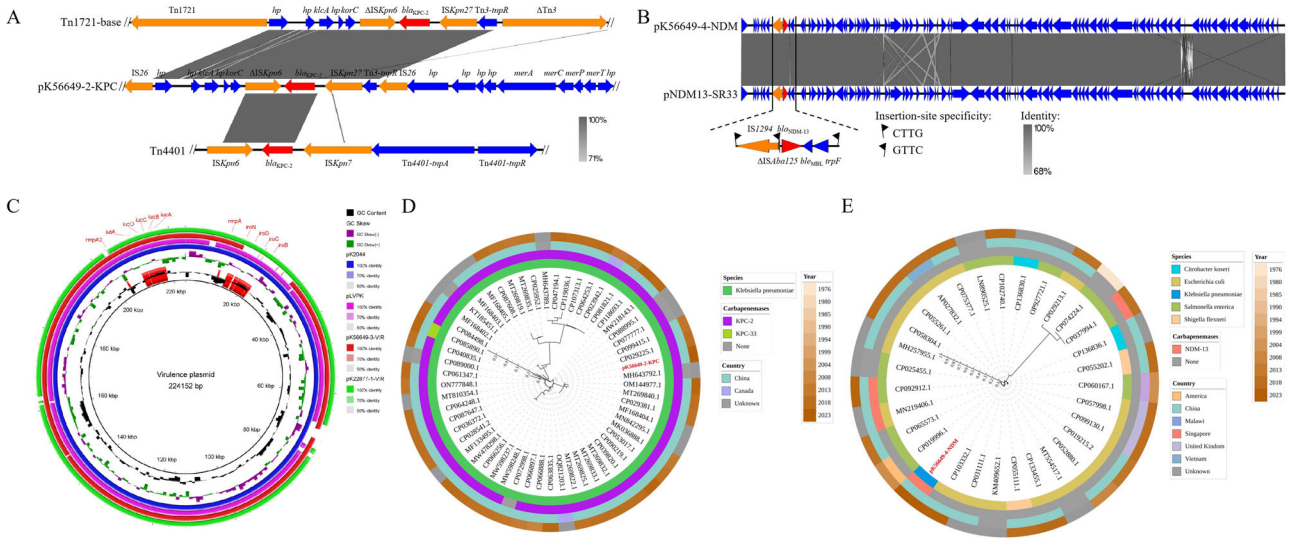

Fig. 3 | Alignment and origin of resistance and virulence plasmids. A Linear alignment of bla_{KPC-2}-bearing structure on pK56649-2-KPC (plasmid of ST11-KL64 hv-CRKP) and two classical surroundings, Tn*1724*-based structure and Tn*4401*. ORFs are indicated by arrows. Sequences of shared homology are marked by grey shading. **B** Linear alignment of bla_{NDM-13}-bearing pK56649-4-NDM of K56649 (the ST11-KL64 hv-CRKP) and pNDM13-SR33 of *Salmonella enterica* SR33. **C** Circular alignment analysis of plasmid pK56649-3-VIR (plasmid of ST11-KL64 hv-CRKP), pK22877-1-VIR (plasmid of ST65-KL2 CR-hvKP) and two classical hypervirulent plasmids, pLVPK and pK2044. Virulence genes were marked by red shading. **D** Maximum-likelihood phylogenetic tree of pK56649-2-KPC and its homological plasmids. **E** Maximum-likelihood phylogenetic tree of pK56649-4-NDM and its homological plasmids. Circles from the inside out showed species, carbapenemase, country and year, and the number in the circle was tree scale.

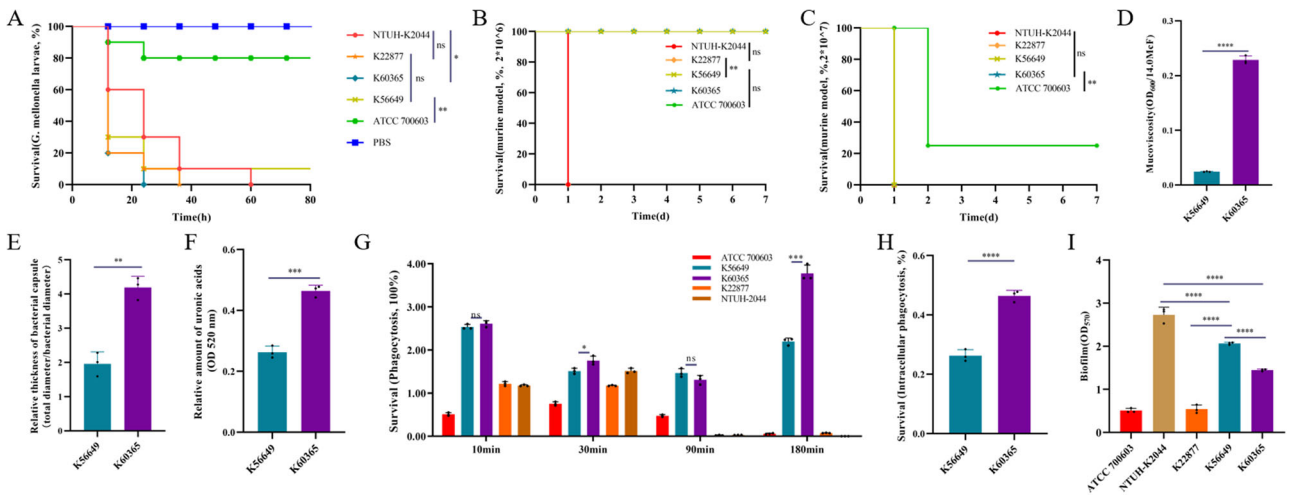

Fig. 4 | Virulence phenotype and diversity of hv-CRKP and CR-hvKP. A The survival rates of K56649 (ST11-KL64 hv-CRKP), K22877 (ST65-KL2 CR-hvKP) and K60365 (ST11-KL64 hv-CRKP) in *G. mellonella* infection model. **B**, **C** Murine model infected with K56649, K22877 and K60365 using different dose (2×10^6 and 2×10^7 CFU, respectively). **D** Mucoviscosity difference between K56649 and K60365. **E**, **F** Comparison of relative thickness and uronic acids content of bacteria capsular between K56649 and K60365. Relative thick was calculated by total diameter/bacterial diameter. **G** Survival rates of K22877, K56649 and K60365 resistance to macrophage phagocytosis. **H** Survival rates of K56649 and K60365 inside of macrophage. **I** Comparison of biofilm formation among K22877, K56649, K60365 and control strains.

phagocytosis and intracellular survival than K56649 ($P < 0.05$, Fig. 4G, H). Therefore, the above-suggested K60365 has a higher level of virulence. Moreover, competitive growth showed K60365 had better growth than K56649 ($w = 5.59 \pm 0.59$). However, biofilm formation analysis demonstrated that the mucoid isolate K60365 had less biofilm than the non-mucoid strain K56649 (Fig. 4I), and growth curve also showed K60365 had fitness cost (Fig. S8A).

Moreover, WGS and S1-PFGE revealed K23016 and K23033 acquired an IncQ resistance plasmid, harboring *aac(6')-Ib-cr*, *aph(3')-Ia*, *aadA1*, *aadA5*, bla_{OXA-1}, bla_{TEM-1B}, $bla_{CTX-M-3}$, *fosA3* and *catB3*, in the process of spread (Fig. S1). Therefore, resistance evolution showed ciprofloxacin resistance was mediated by *aac(6')-Ib-cr* in K23016 and K23033, compared to K22866 (Table 2). There is no significant difference in biological fitness cost between K22877 and K23016 (Fig. S8B).

Similarity and diversity between the two types of hvCRKP

Extensive analysis was conducted to gain a better understanding of the threat that the two hvCRKPs pose to human health (Table 3). ST65-KL2 CR-hvKP originated monophyletically and disseminated only within one hospital across three months. Compared to the CR-hvKP, ST11-KL64 hv-CRKP showed more chains of transmission across different hospitals and continually spread in the hospital within ten months. For resistance, the hv-CRKP contained more resistance genes than the CR-hvKP, which resulted in the dilemma of treating the hv-CRKP. More importantly, infection with

Table 3 | Comprehensive comparison between ST65-KL2 CR-hvKP and ST11-KL64 hv-CRKP in this study

Outbreaks	ST65-KL2 CR-hvKP	ST11-KL64 hv-CRKP
Origination	Monophyletic	Polyphyletic
Transmission	Nosocomial	Nosocomial and regional
Virulence	Hypervirulent	Hypervirulent
Fatality to mice	High	Medium
Resistance	Multi-drug resistant	Extensively-drug resistant
Evolution	Quinolone resistance	Enhanced virulence
Immune status	Immuno-compromised	Immuno-compromised
Dormant infection	None	Existing
Persisting infection	None	Existing
Clearance	Easy	Difficult
Treatment	Aztreonam, Amikacin	Aztreonam/ceftazidime-avibactam
Mortality	40.0%	60.0%

hv-CRKP was difficult to eliminate and sometimes was occult. With regard to virulence, the mortality of mice infected with hv-CRKP (1×10^8 CFU/mL) unit was significantly increased compared with ATCC 700603, while the mortality of mice infected with the hv-CRKP (1×10^7 CFU/mL) showed no statistical significance compared with ATCC 700603 (Fig. 4B, C). However, the CR-hvKP continually maintained higher mortality of mice with different doses strains (10^6, 10^7 and 10^8 CFU/mL)[19]. Correspondently, the virulence of CR-hvKP was stronger than that of hv-CRKP. Moreover, the LD50 of mice injected with hv-CRKP also showed lesser virulence than that of CR-hvKP, according to the summary of the previous studies (Fig. S9A and Table S2). Therefore, we concluded that hv-CRKP generally possessed medium virulence. However, according to clinical outcomes, the hv-CRKP has higher mortality than CR-hvKP (60.0%, 6/10 VS 40.0%, 2/5, respectively).

To better understand the differences of resistance and virulence between ST65-KL2 CR-hvKP and ST11-KL64 hv-CRKP, ST11-KL64 ($n = 2360$) hv-CRKP and ST65-KL2 CR-hvKP ($n = 56$) were retrieved from NCBI, up to December 31, 2023 (Supplementary Data 1 and 2). Carbapenemase genes detection showed ST11-KL64 hv-CRKP was dominated by bla_{KPC-2} (96.9%, 2286/2360), followed by bla_{KPC-2} and bla_{NDM-1} (1.1%, 27/2360) and bla_{KPC-2} and bla_{NDM-5} (0.8%, 18/2360), while ST65-KL2 CR-hvKP was dominated by bla_{KPC-2} (67.9%, 38/56), followed by bla_{NDM-5}(10.7%, 6/56), bla_{IMP-6} (3/56;5.4%) and bla_{IMP-4} (5.4%,3/56). The majority of ST11-KL64 hv-CRKP (96.1%, 2270/2360) had *ybt 9* and *ICEKp3*, whereas the majority of ST65-KL2 CR-hvKP (69.6%, 39/56) had *ybt 17* and *ICEKp10*. Most of ST11-KL64 hv-CRKP (97.9%, 2311/2360) is likely to have OmpK35 truncation/OmpK36GD, according to the OmpK35/36 analysis, while most of ST65-KL2 CR-hvKP (94.6%, 53/56) have normal Ompk35/36, which made the former show higher MICs for carbapenems. The number of resistance genes and their classes hinted that ST11-KL64 hv-CRKP presented an advantage over ST65-KL2 CR-hvKP to acquire exogenous genes easily, but the virulence score is the opposite (Fig. S9B–D). Furthermore, the ratio of wild *rpmA* promotor P_{11T} of ST11-KL64 hvCRKP was 31.9% and significantly lower than that of ST65-KL2 hvCRKP (31.9% VS 71.4%, Fig. S9E).

Discussion

In the past few years, hvCRKP has been increasingly reported globally, particularly in Asia, Europe and America, since the first report of ST23-KL1 bla_{KPC-2}-harboring CR-hvKP isolated from an 85-year-old American with acute myeloid leukemia in 2014[20]. We also reported the emergence of the ST65-KL2 NDM-5-producing hvCRKP, isolated from the BALF of a lung transplant patient in June 2019[19]. Between 2019 and 2023, more than 200 publications concerning hvCRKP in China, accounting for two-thirds of the total worldwide, could be retrieved from PubMed, suggesting hvCRKP was prevalent throughout China and required immediate monitoring and management.

To date, several disseminations of hvCRKP in different hospitals and environments were reported in China, and these strains largely produced carbapenemases KPC and carried hypervirulent plasmids, including ST11-KL47/KL64 hv-CRKP, ST859-K19 hv-CRKP, etc.[14,21]. The proliferation and development of NDM-producing hv-CRKP and CR-hvKP, however, have been rarely documented. Herein, our findings have revealed two outbreaks of divergent evolutionary hvCRKP, ST11-KL64 hv-CRKP and ST65-KL2 CR-hvKP, isolated from patients in critical or transplantation situations in China. All 21 KPC- and NDM-co-producing ST11-KL64 hv-CRKP from the same hospital, belonging to the same clonal cluster, were polyphyletic in origin, and presumably have disseminated regionally due to their specimen collection in the initial hospitalization (≤24 h) from different wards. It was noteworthy that the infections caused by the hv-CRKP either progressed rapidly or recurrently happened in those ten patients. Unlike ST11-KL64 hv-CRKP, whose spreading pathway remained elusive, NDM-producing ST65-KL2 CR-hvKP, a typical hvKP, originated from donor organ and transmitted among five recipients, causing the adverse outcomes of lung transplant recipients and alerting the urgency of anti-infection for patients with the infection of CR-hvKP after solid organ transplantation.

In the present study, the resistance phenotype and genotype analysis revealed ST11-KL64 hv-CRKP, co-carrying bla_{KPC-2} and bla_{NDM-13}, only showed sensitivity to colistin, tigecycline and the combined administration of CZA and aztreonam. However, colistin and tigecycline were not recommended as first-line regimens in CRKP treatment[22], Therefore, in China, considering the accessibility of novel antimicrobial agents, the combination of CZA and aztreonam became the essential medication to address the KPC- and NDM-producing hvCRKP. Compared to ST11-KL64 hv-CRKP, ST65-KL2 CR-hvKP only carried bla_{NDM-5}, and presented simpler resistance genotype. It's worth noting that, in contrast to some bla_{KPC-2}-carrying CR-hvKP, which displayed low-level resistance to carbapenems[23], bla_{NDM-5}-carrying CR-hvKP often demonstrated high-level resistance. Furthermore, bla_{NDM} of the two hvCRKP types, namely, CR-hvKP and hv-CRKP, could be transferred into *E. coli* and *K. pneumoniae via* plasmid, and its genetic surroundings have a potential transferability to cause horizontal spread by forming mobile genetic elements. Although the majority of hvCRKP carried bla_{KPC} and showed good responses to CZA[24,25], the transformation of KPC subtypes, e.g., from bla_{KPC-2} to bla_{KPC-33}, and the acquisition of NDM could cause resistance to CZA during treatment with CZA[26,27].

Both phenotype and genotype are required to identify the hypervirulence in CRKP strains. A series of virulence experiments, including *G. mellonella* infection, murine and macrophage phagocytosis assay, showed both CR-hvKP and hv-CRKP belonged to hypervirulent strains. Generally, the majority of research used different virulence genes and their combinations to define the hypervirulence of *K. pneumoniae*, but lacking experimental validation thus might overstate the incidence of hvCRKP. Accurate and practicable definition of the hypervirulence of hvCRKP remains challenging. Truncation and mutations of hypervirulent genes and the absence and difference of their promotor, such as *rmpA* and *rmpA2*, rendered them non-functional, and the hypervirulent phenotypes will be lost[16]. Comprehensive analysis of the LD50 from previous studies (Table S2) and existing murine model results, revealed CR-hvKP has a more significant virulence phenotype than hv-CRKP. Therefore, compared to CR-hvKP, hv-CRKP might potentially pose a lesser risk of infection and disease severity, which might be coined as "sub-hypervirulent" CRKP. Of course, its reasonability requires further study. Virulent plasmid rarely spreads independently, either collectively transmitted with the help of other self-transferable plasmids that had the maintenance of origin of transfer site (*oriT*) or evolved into self-transferable plasmids by plasmid infusion, including some bla_{KPC-2}-carrying plasmids. It might promote the formation of self-transferrable both carbapenem-resistant and hypervirulent plasmids to accelerate dissemination of hvCRKP[13,23,28].

Evolutionary pathways showed the acquisition of bla_{NDM}-carrying plasmid and hypervirulent plasmid occurred in an opposing manner for the carbapenem-resistant and hypervirulent convergence of the two different hvCRKP. Most CRKP carried bla_{KPC-2}-harboring plasmids in China, and the vertical spread of KPC-producing CRKP and the horizontal spread of conjugative bla_{KPC}-harboring plasmids led to the rise and predominance of CRKP strains in hospitals. Owing to the thick CPS and other constraints, CRKP is more likely to acquire virulence genes than hvKP to obtain resistance genes[29]. Moreover, compared to ST11-KL47, previous studies reported ST11-KL64 hv-CRKP is gradually replacing the former and exhibited greater virulence[30,31]. Compared to CR-hvKP, therefore, hv-CRKP strains, particularly ST11-KL64 hv-CRKP, were better adapted for survival in hospital environments and became prominent hvCRKP[32]. Accurate identification of hvCRKP is a prerequisite of effective treatment strategies. AST and resistance genes help us to use valid antimicrobial agents against hvCRKP. Moreover, hypervirulence alerts the timely and sufficient treatment. In this study, enhanced resistance and virulence were found in the ST65-KL2 CR-hvKP and ST11-KL64 hv-CRKP, respectively, in the process of dissemination. Therefore, timely detection for the change of resistance and virulence is essential, especially for those in critical conditions.

Potential therapeutic approaches and infection control measures should be urgently explored and implemented. Though the ST11-KL64 hv-CRKP in the present study was sensitive to ATM-CZA, it continually existed in bacterial killing assay and proliferated inside macrophages, leading to its intractable removal. Therefore, we should not only use antibiotics against these refractory infections with hvCRKP. In the future, the combined use of immunological regulation, phage therapy, and antibiotics, where much work remains to be done to assist in designing workable solutions, will be more efficient in addressing hvCRKP[33–35]. Besides, a series of prevention and control for infections should be strictly implemented, including physical isolation, handwashing, wearing masks and effective clearance for hvCRKP in the environment and equipment. Effective surveillance strategies for hvCRKP population in healthcare sectors should be rigorously carried out, including active screening for the patients in ICU and transplantation wards.

The present study is limited by several factors. First, the size of ST65-KL2 CR-hvKP and ST11-KL64 hv-CRKP outbreak cases is relatively small within the study period, even though the small sample size is not uncommon in this type of study, therefore reducing the robustness of our study. The conclusions should be interpreted with caution. Second, persistent infection of the ST11-KL64 hv-CRKP was a significant and interesting issue, requiring further study.

In conclusion, the ST65-KL2 CR-hvKP and ST11-KL64 hv-CRKP, having simultaneously hypervirulent and multidrug-resistant, pose an intense ability to disseminate and cause high mortality. Resistance and virulence evolution accelerate a substantial threat to human health. Control measures should be put in place to prevent further dissemination throughout the community and hospital setting. More researches should be focused on the virulence and resistance evolution caused by persistent infection in host and its mechanism in the future.

Methods

Outbreak investigation and its global surveillance for hv-CRKP and CR-hvKP

During our surveillance of CRE isolates, two suspected outbreaks were noted: CR-hvKP strains ($n = 15$), showing positive string test and encoding bla_{NDM-5}, were collected from five patients from June 2019 to August 2019, and hv-CRKP strains ($n = 21$), co-encoding bla_{KPC-2} and bla_{NDM-13}, were collected from ten patients from March 2023 to December 2023. Furthermore, when CRKP strains from the same sample type (e.g., blood, urine, BLAF) of a patient, had identical morphological characteristics and antibiotic susceptibility profiles, only the first isolate was chosen for further study. The demographic characteristics of the patients and detailed information of the above strains were collected.

As described previously[36], species identification was determined by matrix-assisted laser desorption ionization-time of flight mass spectrometry (MALDI-TOF MS) (Bruker Daltonik, Bremen, Germany). Furthermore, to investigate the global prevalence and differences of the above two different types of hvCRKP, ST11-KL64 hv-CRKP ($n = 2360$) and ST65-KL2 CR-hvKP ($n = 56$) were retrieved up to December 31, 2023 from GenBank of the national center for biotechnology information (NCBI). The hvCRKP is genotypically defined as containing the following genes simultaneously: carbapenemase genes, *rmpA* or *rmpA2* and *iutAiucABCD* or *iroBCDN*.

Definition

In the study, hypervirulent and carbapenem-resistant *K. pneumoniae* was defined as hvCRKP. Afterwards we classified hvCRKP as CR-hvKP (hvKP acquiring carbapenem resistance), hv-CRKP (CRKP acquiring hypervirulence) and hvCR-KP (cKP acquiring both hypervirulence and carbapenem resistance), respectively.

Antibiotic sensitivity testing (AST)

Microdilution broth method (bio-KONT, Ltd China) was used to determine the minimal inhibitory concentrations (MICs) of imipenem, meropenem, ceftazidime/avibactam, aztreonam/avibactam, tigecycline and colistin, with *E. coli* ATCC 25922 as the quality control strain[37]. Meanwhile, N335 susceptibility cards and Vitek-2 system (bioMérieux, France) were applied for the MICs of other drugs, including amikacin, aztreonam and ciprofloxacin. The breakpoint of tigecycline was interpreted by the US FDA on AST[38]. The results of other antimicrobial agents were defined following the standards of the Clinical Laboratory Standards Institute (CLSI, 2021)[39]. The production of carbapenemases was evaluated using the carbapenemase inhibitor APB (3-aminophenyl boronic acid) and EDTA enhancement method (APB/EDTA method), as recommended by CLSI 2021[39]. Moreover, High-level carbapenem resistance was defined as the MIC value of meropenem was ≥16 μg/mL, according to the previous study[40].

Whole-genome sequencing and bioinformatic analysis

WGS was performed using Illumina HiSeq 2500 platform for all strains and nanopore sequencing method on MinION flow cells only for K22877, K56649 and K60365. The filtration of raw reads and De novo assembly were conducted using skewer[41], SPAdes Genome Assembler v3.13.1[42] and Unicycler[43]. The antimicrobial resistance, virulence genes, K type and multilocus sequence types (MLST) were identified by Kleborate v2.4.1[44]. The result of Kleborate can be found in Supp Data 3. Plasmid replicon was determined by PlasmidFinder[45] on the CGE server (https://cge.cbs.dtu.dk/services/). The single nucleotide polymorphism (SNP) was performed using Snippy (https://github.com/tseemann/snippy). Linear alignments of bla_{KPC-2}- and bla_{NDM-13}-bearing structures were generated using Easyfig_win_2.1[46]. The comparison of virulence plasmids was determined by the BLAST Ring Image Generator (BRIG) v0.95.22[47]. The transferability of bla_{KPC-2}- and bla_{NDM-13}-carrying plasmids was performed by *oriT*finder[48]. Core genome MLST (cgMLST, 2358 core genes, pairwise ignoring missing values, Ridom SeqSphere+9.0.9 software) and XbaI-Pulsed-field gel electrophoresis (PFGE)[49] were performed to confirm the homology of those strains in the two outbreaks. To trace the origin of pK56649-2-KPC and pK56649-4-NDM, the maximum-likelihood phylogenetic tree of their homological plasmids in this study was built by RaxML[50] from the alignment generated by mafft v7[51]. The homological plasmids from global strains were defined that plasmids from nucleotide BLAST database (nr/nt) of NCBI have ≥95% identity and coverage with pK56649-2-KPC and pK56649-4-NDM *via* online sequence blasting. The iTOL (https://itol.embl.de) was used for visualization. To understand the diversities of two different types of hvCRKP, *rmpA* and its promotor were abstracted from genomes of ST11-KL64 hv-CRKP ($n = 2360$) and ST65-KL2 CR-hvKP ($n = 56$), and were compared with that of hypervirulent pLVKP (AY378100.1) by using BLAST + 2.14.0.

Plasmid conjugation assays and fitness cost

Plasmid conjugation experiments were performed for *K. pneumoniae* strains K22877 and K56649. Azide-resistant *E. coli* J53 and amikacin-resistant *K. pneumoniae* KP54 were applied as the recipient strains. Briefly, both donor and recipient were adjusted to a McFarland standard of 0.5 and mixed at a ratio of 1:3, and after 18-h incubation at 37 °C, the mixture was selected on China blue agar (CBA) plates containing both meropenem (1 mg/L) and amikacin (16 mg/L) or azide (120 mg/L). The above trans-conjugants were confirmed by PCR and AST.

To evaluate the fitness cost of the evolutionary strains, the growth curve assay was performed. Growth curves of K22877 with K23033 and K56649 with K60365 were measured during the exponential growth phase as the maximum increase in optical density over time, as previously described[52]. Competitive growth test was used to estimate relative fitness of K56649 and K60365 with different mucoid phenotypes on CBA[53]. Briefly, equal volumes (10 μL) of overnight cultures of hypermucoid K60365 and regular-mucoid K56649 were mixed and added into 5 mL fresh LB broth to grow competitively for 24 h. Then 20 μl of overnight culture was added into 5 mL fresh LB broth to grow again for 24 h. The cultures were serially diluted using PBS and grown on antibiotic-free CBA agar. Bacteria with different mucoid phenotypes were distinguished by morphologies and string tests. Relative fitness (w) was calculated using this formula, $w = \log_{10}(N1_{48}/N1_0)/\log_{10}(N2_{48}/N2_0)$, where N1 and N2 are defined as the number of K60365 and K56649, respectively. $w < 1$ suggests a fitness cost, while $w > 1$ suggests a fitness advantage. Each experiment was repeated in triplicate.

Virulence evaluation

Galleria mellonella infection model and murine model were performed as described previously[54]. Briefly, for *G. mellonella*, exponential growth phase bacteria cultures (37 °C, 200 rpm, 4 h) were washed with sterile PBS and then adjusted to a McFarland standard of 0.5. Suspension was thereafter diluted to 1×10^7 CFU/mL. Ten larvae were injected with 10 μL above bacterial suspension and PBS as control, and then incubated at 37 °C in darkness for 72 h. The dead larvae were counted per 12 h. For murine model, single colonies of *K. pneumoniae* isolates, including hypervirulent strain NTUH-K2044 and hypovirulent strains ATCC 700603, were grown in LB broth, and diluted to 1×10^7 and 1×10^8 CFU/mL with sterile PBS. Female BALB/c mice (6–8 weeks,18–20 g and each group of four mice) were injected with the above stains at 200 μL by intraperitoneal injection. The dead mice were counted for 7 days after infection. The experiment was performed in triplicate. The log-rank test was performed using GraphPad Prism 6. Ethics oversight: All animal experiments were conducted following institutional ethics requirements under China-Japan Friendship Hospital (CJFH) approved this study (2022-KY-054). We have complied with all relevant ethical regulations for animal use.

To estimate the differences of virulence between K56649 and K60365, mucoviscosity assay, capsular thickness, biofilm formation and uronic acids, were conducted as performed previously[54]. Briefly, mucoviscosity assay was performed by measuring the OD_{600} of bacteria supernatant, which was obtained by centrifuging bacteria cultures overnight (MCF = 14.0) for 5 min at 2000 rpm. Capsular was distinguished by ink staining, and relative capsular thickness was measured by total diameter/bacterial diameter. Uronic acids was extracted as performed previously[54] and was measured by OD_{520}. Moreover, biofilm of bacteria culture in 96-well polystyrene plates was stained with 0.1% crystal violet at room temperature for 20 min, as described previously[54].

Macrophage phagocytosis assay was performed to evaluate the phagocytosis resistance of hvCRKP with slight modification[54]. Briefly, RAW264.7 macrophages in DEME were infected with 2×10^6 (MOI = 5) hvCRKP and the control strains NTUH-K2044 and ATCC 700603. After incubation with the above bacteria for 10 min, 30 min, 90 min and 180 min, respectively, the cells were then gently washed three times with PBS and lysed with 0.2% Triton X-100, and the survival bacteria were diluted and cultured onto CBA agar overnight to count, as described previously[54].

Bacterial survival rate was calculated as follows: = Number of bacteria in the experiment group/Number of bacteria in the control group.

Intracellular bacteria killing was also performed. The incubation with RAW264.7 and K56649 or K60365 for 30 min was exposed to tigecycline (128 mg/L) to kill extracellular bacteria for one hour. The above incubation was washed three times with PBS and then cultured one hour to compare the relative survival rate. The experiments were conducted in triplicates.

Statistics and reproducibility

GraphPad Prism 8.2.1 was used for data analyses. Data are expressed as mean ± standard deviation. Significant differences were assessed using a one-way analysis of variance, with $P < 0.05$ being considered statistically significant.

Reporting summary

Further information on research design is available in the Nature Portfolio Reporting Summary linked to this article.

Data availability

Complete sequences of K22877, K56649 and K60365 were deposited to National Center for Biotechnology Information (NCBI) in BioProject: PRJNA1102845. Supplementary data to this article can be found in the appendix as separate Excel files.

Received: 8 July 2024; Accepted: 22 November 2024;
Published online: 02 December 2024

References

1. Navon-Venezia, S., Kondratyeva, K. & Carattoli, A. Klebsiella pneumoniae: a major worldwide source and shuttle for antibiotic resistance. *FEMS Microbiol. Rev.* **41**, 252–275 (2017).
2. Cassini, A. et al. Attributable deaths and disability-adjusted life-years caused by infections with antibiotic-resistant bacteria in the EU and the European Economic Area in 2015: a population-level modelling analysis. *Lancet Infect. Dis.* **19**, 56–66 (2019).
3. Paniagua-Garcia, M. et al. Attributable mortality of infections caused by carbapenem-resistant Enterobacterales: results from a prospective, multinational case-control-control matched cohorts study (EURECA). *Clin. Microbiol. Infect.* **30**, 223–230 (2024).
4. Russo, T. A. & Marr, C. M. Hypervirulent Klebsiella pneumoniae. *Clin. Microbiol. Rev.* **32**, e00001–19 (2019).
5. Russo, T. A. et al. Identification of biomarkers for differentiation of hypervirulent Klebsiella pneumoniae from classical K. pneumoniae. *J. Clin. Microbiol.* **56**, e00776–18 (2018).
6. Kochan, T. J. et al. Klebsiella pneumoniae clinical isolates with features of both multidrug-resistance and hypervirulence have unexpectedly low virulence. *Nat. Commun.* **14**, 7962 (2023).
7. Wyres, K. L., Lam, M. M. C. & Holt, K. E. Population genomics of Klebsiella pneumoniae. *Nat. Rev. Microbiol.* **18**, 344–359 (2020).
8. Walker, K. A. & Miller, V. L. The intersection of capsule gene expression, hypermucoviscosity and hypervirulence in Klebsiella pneumoniae. *Curr. Opin. Microbiol.* **54**, 95–102 (2020).
9. Heng, H. et al. Global genomic profiling of Klebsiella pneumoniae: a spatio-temporal population structure analysis. *Int. J. Antimicrob. Agents* **63**, 107055 (2024).
10. Emeraud, C. et al. Emergence and rapid dissemination of highly resistant NDM-14-producing Klebsiella pneumoniae ST147, France, 2022. *Eur. Surveill.* **28**, 2300095 (2023).
11. Lapp, Z. et al. Regional spread of blaNDM-1-containing Klebsiella pneumoniae ST147 in post-acute care facilities. *Clin. Infect. Dis.* **73**, 1431–1439 (2021).
12. Di Pilato, V. et al. Resistome and virulome accretion in an NDM-1-producing ST147 sublineage of Klebsiella pneumoniae associated with an outbreak in Tuscany, Italy: a genotypic and phenotypic characterisation. *Lancet Microbe*. **3**, e224–e234 (2022).

13. Yang, X., Dong, N., Chan, E. W., Zhang, R. & Chen, S. Carbapenem resistance-encoding and virulence-encoding conjugative plasmids in Klebsiella pneumoniae. *Trends Microbiol.* **29**, 65–83 (2021).
14. Gu, D. et al. A fatal outbreak of ST11 carbapenem-resistant hypervirulent Klebsiella pneumoniae in a Chinese hospital: a molecular epidemiological study. *Lancet Infect. Dis.* **18**, 37–46 (2018).
15. Liu, L. et al. Chasing the landscape for intrahospital transmission and evolution of hypervirulent carbapenem-resistant Klebsiella pneumoniae. *Sci. Bull.* **68**, 3027–3047 (2023).
16. Yang, X. et al. Molecular epidemiology of carbapenem-resistant hypervirulent Klebsiella pneumoniae in China. *Emerg. Microbes Infect.* **11**, 841–849 (2022).
17. Tang, Y., Li, G., Shen, P., Zhang, Y. & Jiang, X. Replicative transposition contributes to the evolution and dissemination of KPC-2-producing plasmid in Enterobacterales. *Emerg. Microbes Infect.* **11**, 113–122 (2022).
18. Ma, K., Feng, Y., McNally, A. & Zong, Z. Hijacking a small plasmid to confer high-level resistance to aztreonam-avibactam and ceftazidime-avibactam. *Int. J. Antimicrob. Agents* **62**, 106985 (2023).
19. Zhao, J. et al. Characterization of an NDM-5-producing hypervirulent Klebsiella pneumoniae sequence type 65 clone from a lung transplant recipient. *Emerg. Microbes Infect.* **10**, 396–399 (2021).
20. Cejas, D. et al. First isolate of KPC-2-producing Klebsiella pneumonaie sequence type 23 from the Americas. *J. Clin. Microbiol.* **52**, 3483–3485 (2014).
21. Zhu, J., Jiang, X., Zhao, L. & Li, M. An Outbreak of ST859-K19 carbapenem-resistant hypervirulent Klebsiella pneumoniae in a Chinese Teaching Hospital. *mSystems* **7**, e0129721 (2022).
22. Tamma, P. D. et al. Infectious Diseases Society of America 2024 guidance on the treatment of antimicrobial-resistant gram-negative infections. *Clin. Infect. Dis.* **7**, ciae403 (2024).
23. Zhou, Y. et al. Characterization difference of typical KL1, KL2 and ST11-KL64 hypervirulent and carbapenem-resistant Klebsiella pneumoniae. *Drug Resist. Updat.* **67**, 100918 (2023).
24. Guo, M. Q. et al. Genomic epidemiology of hypervirulent carbapenem-resistant Klebsiella pneumoniae at Jinshan local hospital, Shanghai, during 2014-2018. *J. Microbiol. Immunol. Infect.* **57**, 128–137 (2024).
25. Wu, Y. et al. Global evolution and geographic diversity of hypervirulent carbapenem-resistant Klebsiella pneumoniae. *Lancet Infect. Dis.* **22**, 761–762 (2022).
26. Zhang, Y., Tian, X., Fan, F., Wang, X. & Dong, S. The dynamic evolution and IS26-mediated interspecies transfer of a bla(NDM-1)-bearing fusion plasmid leading to a hypervirulent carbapenem-resistant Klebsiella pneumoniae strain harbouring bla(KPC-2) in a single patient. *J. Glob. Antimicrob. Resist.* **35**, 181–189 (2023).
27. Zhang, P. et al. Emergence of bla(KPC-33)-harboring hypervirulent ST463 Pseudomonas aeruginosa causing fatal infections in China. *J. Infect.* **85**, e86–e88 (2022).
28. Xu, Y. et al. Mobilization of the nonconjugative virulence plasmid from hypervirulent Klebsiella pneumoniae. *Genome Med.* **13**, 119 (2021).
29. Wyres, K. L. et al. Distinct evolutionary dynamics of horizontal gene transfer in drug resistant and virulent clones of Klebsiella pneumoniae. *PLoS Genet.* **15**, e1008114 (2019).
30. Xie, M. et al. Clinical use of tigecycline may contribute to the widespread dissemination of carbapenem-resistant hypervirulent Klebsiella pneumoniae strains. *Emerg. Microbes Infect.* **13**, 2306957 (2024).
31. Zhou, K. et al. A point mutation in recC associated with subclonal replacement of carbapenem-resistant Klebsiella pneumoniae ST11 in China. *Nat. Commun.* **14**, 2464 (2023).
32. Tian, D. et al. Prevalence of hypervirulent and carbapenem-resistant Klebsiella pneumoniae under divergent evolutionary patterns. *Emerg. Microbes Infect.* **11**, 1936–1949 (2022).
33. Fajardo-Lubian, A. & Venturini, C. Use of bacteriophages to target intracellular pathogens. *Clin. Infect. Dis.* **77**, S423–S432 (2023).
34. Li, J. et al. Development of phage resistance in multidrug-resistant Klebsiella pneumoniae is associated with reduced virulence: a case report of a personalised phage therapy. *Clin. Microbiol. Infect.* **29**, e1601–e1607 (2023).
35. Eskenazi, A. et al. Combination of pre-adapted bacteriophage therapy and antibiotics for treatment of fracture-related infection due to pandrug-resistant Klebsiella pneumoniae. *Nat. Commun.* **13**, 302 (2022).
36. Lu, B. et al. Listeriosis cases and genetic diversity of their L. monocytogenes Isolates in China, 2008-2019. *Front. Cell Infect. Microbiol.* **11**, 608352 (2021).
37. Zhao, J. et al. Convergence of MCR-8.2 and chromosome-mediated resistance to colistin and tigecycline in an NDM-5-Producing ST656 Klebsiella pneumoniae isolate from a lung transplant patient in China. *Front. Cell Infect. Microbiol.* **12**, 922031 (2022).
38. Marchaim, D. et al. Major variation in MICs of tigecycline in Gram-negative bacilli as a function of testing method. *J. Clin. Microbiol.* **52**, 1617–1621 (2014).
39. CLSI. Performance standards for antimicrobial susceptibility testing. 34sted. CLSI supplement M100. Wayne, PA: Clinical and Laboratory Standards Institute. (2024).
40. Satlin, M. J. et al. Multicenter clinical and molecular epidemiological analysis of bacteremia due to carbapenem-resistant enterobacteriaceae (CRE) in the CRE epicenter of the United States. *Antimicrob. Agents Chemother.* **61**, e02349–16 (2017).
41. Jiang, H., Lei, R., Ding, S. W. & Zhu, S. Skewer: a fast and accurate adapter trimmer for next-generation sequencing paired-end reads. *BMC Bioinform.* **15**, 182 (2014).
42. Prjibelski, A., Antipov, D., Meleshko, D., Lapidus, A. & Korobeynikov, A. Using SPAdes De Novo assembler. *Curr. Protoc. Bioinform.* **70**, e102 (2020).
43. Wick, R. R., Judd, L. M., Gorrie, C. L. & Holt, K. E. Unicycler: resolving bacterial genome assemblies from short and long sequencing reads. *PLoS Comput. Biol.* **13**, e1005595 (2017).
44. Lam, M. M. C. et al. A genomic surveillance framework and genotyping tool for Klebsiella pneumoniae and its related species complex. *Nat. Commun.* **12**, 4188 (2021).
45. Carattoli, A. et al. In silico detection and typing of plasmids using PlasmidFinder and plasmid multilocus sequence typing. *Antimicrob. Agents Chemother.* **58**, 3895–3903 (2014).
46. Sullivan, M. J., Petty, N. K. & Beatson, S. A. Easyfig: a genome comparison visualizer. *Bioinformatics* **27**, 1009–1010 (2011).
47. Alikhan, N. F., Petty, N. K., Ben Zakour, N. L. & Beatson, S. A. BLAST Ring Image Generator (BRIG): simple prokaryote genome comparisons. *BMC Genomics* **12**, 402 (2011).
48. Li, X. et al. oriTfinder: a web-based tool for the identification of origin of transfers in DNA sequences of bacterial mobile genetic elements. *Nucleic Acids Res.* **46**, W229–W234 (2018).
49. Wang, X. et al. Emergence of a novel mobile colistin resistance gene, mcr-8, in NDM-producing Klebsiella pneumoniae. *Emerg. Microbes Infect.* **7**, 122 (2018).
50. Stamatakis, A. RAxML version 8: a tool for phylogenetic analysis and post-analysis of large phylogenies. *Bioinformatics* **30**, 1312–1313 (2014).
51. Katoh, K., Rozewicki, J. & Yamada, K. D. MAFFT online service: multiple sequence alignment, interactive sequence choice and visualization. *Brief. Bioinform.* **20**, 1160–1166 (2019).
52. Gao, H. et al. The transferability and evolution of NDM-1 and KPC-2 co-producing Klebsiella pneumoniae from clinical settings. *eBioMedicine* **51**, 102599 (2020).
53. Zhang, B. et al. Comparison of two distinct subpopulations of Klebsiella pneumoniae ST16 co-occurring in a single patient. *Microbiol. Spectr.* **10**, e0262421 (2022).
54. He, J. et al. Opposite evolution of pathogenicity driven by in vivo wzc and wcaJ mutations in ST11-KL64 carbapenem-resistant Klebsiella pneumoniae. *Drug Resist. Updat.* **66**, 100891 (2023).

Acknowledgements
The authors would like to acknowledge the support of National Center for Respiratory Medicine. This work was supported by Beijing Natural Science Foundation (7242124) and the CAMS Innovation Fund for Medical Sciences (CIFMS; No.2021-I2M-1-030).

Author contributions
Z.F.L.: Writing - original draft & review & editing, Software, Methodology, Formal analysis and Data curation. L.Z.H. & L.Z.Y.: Software and Methodology. L.X.M. & L.Z.C.: Data curation and Methodology. Z.X.X. and Y.X.R.: Methodology. Z.J.K. & Z.Y.L.: Writing - review & editing. L.H.B.: Writing - review & editing, Visualization, Supervision, Project administration, Conceptualization and Funding acquisition.

Competing interests
The authors declare no competing interests.

Ethics approval
The Ethics Committee of the China-Japan Friendship Hospital (CJFH) approved this study (2022-KY-054) and waived the necessity of informed consent due to the observational nature of the study with the guarantee of anonymous data collection. All in vivo animal studies were in line with ethically and regulatory requirements and approvals.

Additional information
Supplementary information The online version contains supplementary material available at https://doi.org/10.1038/s42003-024-07310-2.

Correspondence and requests for materials should be addressed to Binghuai Lu.

Peer review information *Communications Biology* thanks Varun Shamanna, Polly Yap and the other, anonymous, reviewer(s) for their contribution to the peer review of this work. Primary Handling Editor: Tobias Goris.